Superlubricity mechanism of diamond-like carbon with glycerol. Coupling of experimental and simulation studies

M I De Barros Bouchet [1], C Matta [1], Th. Le-Mogne[1], J Michel Martin [1], Q Zhang [2], W Goddard III [2], M Kano [3], Y Mabuchi[4] and J Ye [5]

[1] Laboratory of Tribology and System Dynamics,Ecole Centrale de Lyon, 69134 Ecully, France
[2] Materials and Process Simulation Center, California Institute of Technology, Pasadena CA, USA
[3] Nissan Research Center, to Kanagawa Industrial Technology Center, 705-1， 1 Shimo-imaizumi, Ebina, Kanagawa 243-0435, Japan
[4] Materials Engineering Department, Nissan Motor Co., Ltd., 6-1,Daikoku-cho, Tsurumi-ku, Yokohama, Japan
[5] Research Department, NISSAN ARC LTD., 1 Natsushima-cho, Yokosuka 237-8523, Japan

E-mail corresponding author: maria-isabel. de-barros@ec-lyon.fr

Abstract. We report a unique tribological system that produces superlubricity under boundary lubrication conditions with extremely little wear. This system is a thin coating of hydrogen-free amorphous Diamond-Like-Carbon (denoted as ta-C) at 353 K in a ta-C/ta-C friction pair lubricated with pure glycerol. To understand the mechanism of friction vanishing we performed ToF-SIMS experiments using deuterated glycerol and ^{13}C glycerol. This was complemented by first-principles-based computer simulations using the ReaxFF reactive force field to create an atomistic model of ta-C. These simulations show that DLC with the experimental density of 3.24 g/cc leads to an atomistic structure consisting of a 3D percolating network of tetrahedral (sp^3) carbons accounting for 71.5% of the total, in excellent agreement with the 70% deduced from our Auger spectroscopy and XANES experiments. The simulations show that the remaining carbons (with sp^2 and sp^1 character) attach in short chains of length 1 to 7. In sliding simulations including glycerol molecules, the surface atoms react readily to form a very smooth carbon surface containing OH-terminated groups. This agrees with our SIMS experiments. The simulations find that the OH atoms are mostly bound to surface sp^1 atoms leading to very flexible elastic response to sliding. Both simulations and experiments suggest that the origin of the superlubricity arises from the formation of this OH-terminated surface.

1 Introduction

1.1 Survey on Extremely low Friction under boundary lubrication

Systematic research on friction started with Leonardo da Vinci (1516). The traditional Amonton friction law $F=\mu N$ relates the friction force F to the normal load via the friction coefficient μ. The Bowden and Tabor model of friction provides a good starting point for understanding how a thin interface film can drastically reduce the friction coefficient [1]. The friction coefficient is assumed to depend on the normal load W, the real contact area A and the shear strength S of the interfacial tribofilm (or film transfer) as:

$$\mu = S\frac{A}{W} \qquad (1)$$

The shear strength S of solids at high pressure is generally observed to be pressure dependent, which can be approximated by [2]:

$$S = S_0 + \alpha P \quad (2)$$

According to the Hertzian contact theory (below the elastic limits), and in the sphere-on-plane configuration, the friction coefficient μ depends of three variables as [3]:

$$\mu = S_0 \pi \left(3R/4E\right)^{2/3} W^{-1/3} + \alpha \quad (3)$$

Where E is the composite elastic modulus of the contacting materials and R is the radius of the sphere. This simplified model assumes that the real contact area corresponds to the Hertzian zone, as calculated in equation (3). This assumption has been verified for soft and very thin interface films that lead to good accommodation in the contact geometry. Therefore, friction measurements at different normal loads can be useful to determine S_0 and α values in a given tribological system. However, equation (3) indicates that the minimum friction coefficient value is α so that the friction cannot vanish completely. For example friction experiments performed on MoS_2 coatings under different atmospheres [4-8] have led to α =0.001. On the other hand, if the shear strength of the interface is very low, say 25 MPa, μ is predicted to be a few thousandths (μ< 0.01) making the measurement of friction very difficult. The accuracy of mechanical devices measuring the friction tangential force and the normal load simultaneously makes it difficult to quantify the friction for μ< 0.01, which we refer to as extremely low friction or superlubricity.

In the case of very thin interface films such as H-terminated surfaces on carbon materials, or very thin tribofilms (thickness below 2 nm), it is not certain that equations (2) and (3) are still valid and the existence of a limiting value to the lowest friction attainable remains questionable.

1.2. Superlubricity of MoS_2 and DLC

The macroscopic friction laws in equations (1)-(3) result from the combined response of many microcontacts, which, in turn, constitute an ensemble of nanoscale contacts. Probably the most fundamental question in tribology concerns the route via which energy is dissipated in the contacts. Superlubricity (the vanishing of friction force) was predicted theoretically by Hirano [9] in 1991 based on frictional anisotropy between incommensurate crystal surfaces. This prediction was verified experimentally by some of the authors [4-8]. Thus in 1993 the friction coefficient on pure molybdenum disulphide (MoS_2) coatings was shown experimentally to become immeasurably small (i.e., below 0.002) in an ultrahigh vacuum [4]. High-resolution transmission electron microscopic (TEM) investigations [4] showed that the super low friction behavior probably has a structural origin, arising from the frictional anisotropy between rotated MoS_2 nanocrystals in the contact area. In 2000, Chhowalla and Amaratunga [10] reported similar ultralow friction and wear performance for a fullerene-like MoS_2 nanoparticle material. It was later discovered by several authors independently that some hydrogenated diamond-like carbon (DLC) coatings exhibit the same super low state with a friction coefficient lying in the millirange [11]. The super low friction property was obtained when sliding a DLC surface (a-C:H) containing a large amount of hydrogen (more than 40 atomic %) on steel (or the same DLC material) in an ultrahigh vacuum or in a dry inert gas atmosphere [11, 12]. Previous results indicated that hydrogen plays a dominant role in the friction behavior of a-C:H films [13, 14]. Here the formation of a transfer film on the steel counterface seems a necessary condition [15]. The resulting topcoats were suggested to interact through weak van der Waals forces and repulsive electrostatic forces due to positively charged H-terminated carbon atoms [14]. It is plausible that friction between H-terminated carbon surfaces would be low because the C-H/C-H interface has a low binding energy of 0.08 eV per bond. According to the model in equation (3), the shear strength of 10 MPa expected for such a system would lead to a steady-state friction coefficient lower than 0.01 [14].

Such systems with super low friction are certainly of great interest to address tribological issues for space applications, but for industrial machines, it is the friction under the boundary lubrication conditions that is relevant. We report here the first example of super low friction for such systems.

2. Methods

2.1. Sliding test experiments

The pin-on-disc sliding tests were conducted in the following manner. The pins, measuring 5 mm in diameter and 5 mm in length, were made of hardened bearing steel (AISI 52100) and polished to a surface roughness of Ra 0.05 micron. The disc measured 35 mm in diameter and 2.5 mm in thickness and was made of carburized steel. The three pins were secured to prevent them from rotating and were pressed against the toric sliding surface of the rotating disc at a position that was 20 mm in diameter from the center of the disc. Contact at the sliding interfaces was in the shape of lines under high Hertzian pressure of 700 MPa. Lubrication was provided by an oil bath heated to 353 K. The sliding speed was varied in a range of 0 to 1 m/s for the results in figure 1.

The SRV sliding tests were performed with a reciprocating, needle-pin-on-flat-disc tribometer that was lubricated before the test by wetting it with several droplets (5 cc) of the test oil heated to 353 K. The pins, measuring 18 mm in diameter and 22 mm in length, were made of hardened steel and polished to a surface roughness of Ra 0.05 micron. The disc measured 24 mm in diameter and 7.9 mm in thickness and was made of carburized steel. The reciprocating pins were pressed against the stationary disc by a force of 400 N that generated 270 MPa of pressure. The length of the track was 3.0 mm and the reciprocating time was 15 minutes at 50 Hz.

2.2. DLC coating preparation

The ta-C DLC coating was applied to the polished carburized steel disc and the hardened steel pins to a thickness of 0.5 micron from a graphite target by arc-ion plating, a physical vapor deposition (PVD) process, and did not contain hydrogen. The hydrogen-containing DLC (a-C:H) coating was applied to the polished carburized steel disc and hardened steel pins to a 1.0-micron thickness by a plasma-assisted chemical vapor deposition (CVD) process from hydrocarbon gas and contained about 20 at% of hydrogen.

2.3. Surface analysis experiments

X-ray Photoelectron Spectroscopy (XPS) and X-ray Excited Auger Electron Spectroscopy (XAES) data were obtained using a VG 220I apparatus. XPS was performed with a non-monochromatized source that had a dual anode for MgKα or AlKα irradiation. The size of the X-ray probe was set at 100 $\times$100 μm^2 so that well spatially resolved analysis can be achieved. XAES spectra were recorded with the 0.5$\times$0.5 μm^2 focused electron beam which permits a high spatial resolution. Special attention has been paid to the Auger C_{KLL} line to obtain a good signal/noise ratio. Interestingly, the thickness probed in XPS and XAES is about 5 nm with the exponential decay.

Time of Flight-Secondary Ion Mass Spectrometry (ToF-SIMS) experiments were performed with a ToF-SIMS V apparatus from ION-TOF. For static Static SIMS analysis (SSIMS), Au^+ pulsed ion beam of 25 KeV energy was used for scanning an area of 100 $\times$100 μm^2 on the surface. The diameter of the spot was smaller than 1 μm in order to obtain average information. In SSIMS, chemical information is coming from a depth of 0.1-1 nm below the surface. This is much more near-surface information than the one obtained with XPS and XAES techniques. With pure ^{13}C glycerol (^{13}C G) and deuterated glycerol (^{2}H G) lubricants, SSIMS spectra were recorded inside and outside the tribofilm area to clarify the material change on the ta-C surface *after* the super low friction tests.

For Dynamic SIMS (DSIMS), depth profiles were obtained combining depth profiling with secondary ion analysis. Sputter erosion was achieved using O_2^+ ions low energy beam of 0.5 KeV. Analysis of the crater centre was performed using Ga+ ions high-energy beam of 15 KeV.

Before surface analysis, all samples tested in friction were cleaned with heptane in ultrasonic bath for 15 minutes. It is important to mention that the glycerol mono-oleate (GMO) and glycerol are not soluble in heptane but are emulsified with an ultrasonic bath.

2.4. FIB preparation and TEM study

Transmission Electron Microscopy sample was prepared by Focused Ion Beam technique. A transversal cut of ta-C sample was performed to obtain a 100 nm thick cross-section of the coating. To preserve the top of coating, a W layer was previously deposited on the DLC coating before nanomachining by a Ga+ ion beam. Energy Filtered TEM experiments were performed on a LEO 912 energy-filtering equipped with a cold stage holder, in order to avoid irradiation damage. The microscope equipped with an omega energy filter was operating with an accelerating voltage of 120 kV. EELS spectra in the nanoprobe mode (spot size of 0.5 nm) were acquired using a JEOL 2010F operating with a 200 kV accelerating voltage. FIB samples were also observed using a FEI XL 30 ESEM FEG operating in vacuum (accelerating voltage of 30kV). Observations were performed using secondary electron (SE) detector to obtain a topographic image of the FIB preparation, or in the transmission mode to compare results obtained with the other accelerating voltages (200 kV and 120 kV).

2.5. Computer simulation methods.

These studies used the ReaxFF reactive force field based on quantum mechanics studies of structures and reactions of many carbon-based systems [16]. Previous studies have documented the accuracy of ReaxFF to describe reactions and to prepare structures for amorphous systems [17].

2.5.1. The atomistic structure of Bulk ta-C DLC. In order to obtain an amorphous carbon structure from simulations, we started with a periodic cell containing 512 atoms in the diamond structure (4×4×4 superlattice), heated this system to 8000K for 2 ps to form the liquid phase, then quenched the system to 300 K at a cooling rate of 1400 and 100 K/ps, and finally equilibrated the structure at 300 K for 3 ps. The process was carried out for densities ranging from 2.7 to 3.4g/cm^3, leading to different energies. We found that lower cooling rates decrease the energy of DLC structures, leading to stable DLC structures with densities of 3.0 to 3.3g/cm^3. In this study, we discuss the 3.24 g/cc system (the experimental value).

2.5.2. Surface of ta-C DLC. To construct the surface of DLC, we cut through the cell with planes perpendicular to each of the x, y, and z direction. For each direction, we attempted to cut the solid at 40 places, equally spaced at 0.5 Å and spanning the periodic supercell of 14.75 Å. In each case, the two parts of the DLC were first separated by 1.5 Å and the positions of the atoms optimized to minimize the ReaxFF energy. Then we selected the plane with the lowest energy from each of the three sets and carried out MD at 300K while separating the planes by a total of 2.5 Å. Then we selected the best of these cases as the actual surface of this particular DLC structure. The results discuss one of these cases.

2.5.3. Computer Simulations of the frictional properties of lubricated surfaces of ta-C DLC. Using this surface we carried out MD simulations using ReaxFF, while sliding the top surface with respect to the bottom one [18, 19].

The ta-C/ta-C sliding couple was constructed by bringing two ta-C DLC slabs into contact. Periodic boundary conditions were imposed in the x-y plane, while about 45-48 Å of vacuum was allowed in the z direction. The bottom 0.9 Å of the lower slab (with 32 atoms per cell) were held rigid in all simulations

while the top 0.9 Å of the upper slab was slid at a constant velocity of 1nm/ps along the sliding direction. At each point, all remaining 480 atoms were allowed to move freely according to the forces. An external force was imposed along the z direction (perpendicular to the slabs) to keep the distance between the centers of mass of the two slabs constant. This provides the normal load.

Starting with the initial interface models at an initial temperature of 300 K we carried out constant energy MD simulations while keeping the cell parameters fixed (NVE). These calculations were carried out under a number of conditions including:

a) bare ta-C surfaces ;
b) introduction of 6 glycerol molecules to form a monolayer at the interface between ta-C surfaces,

3. Results and Discussion

We evaluated the friction properties under boundary lubrication conditions for more than 50 different kinds of DLC coating materials, including: hydrogen-containing DLC (a-C:H), metal-containing DLC (Me-C:H), and hydrogen-free DLC (a-C and ta-C). We found that the best performance is for hydrogen-free DLC (ta-C), which we focus on here.

3.1. Friction of Steel/DLC in presence of Glycerol Mono-Oleate (GMO)

We evaluated the effect of the friction-modifier additive glycerol mono-oleate (GMO) on the friction property of ta-C, when added in a poly-alpha-olefin (PAO) base oil. First, tribological tests were conducted using a pin-on-disc type machine consisting of three fixed pins sliding on a rotating disc as a function of the sliding speed (figure 1). The results are compared with those obtained with the a-C:H/steel pair in the same conditions and the results found for a needle bearing lubricated with 5W-30 engine oil. The results in figure 1 show that the friction coefficients of the ta-C/steel pairs are much lower than those of the a-C:H/steel pairs. Most notable here is that the ta-C/steel pair lubricated with PAO+GMO exhibited a super low friction coefficient of 0.006 at sliding speeds over 0.1 m/s (100 rpm), which is comparable to the friction coefficient of the needle bearing (pure rolling). This super low friction performance demonstrates for the first time that the rolling contact friction level of needle bearings can be obtained in sliding contact. The substantially lower friction coefficient observed for this material is consistent with the formation of a low-shear-strength tribofilm resulting from reactions of ta-C with GMO that might be formed on the hydrogen-free ta-C surface. To establish whether this is the case, we carried out experiments and computer simulations, as described below.

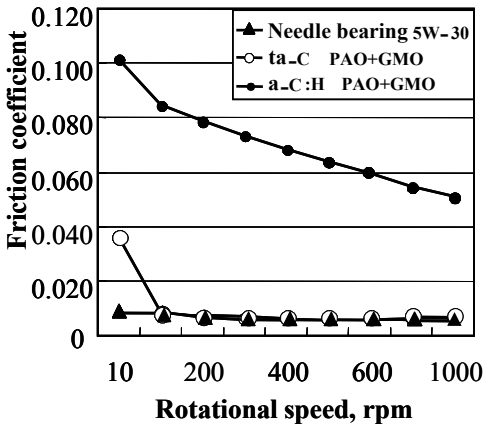

Figure 1: Friction properties of the ta-C/steel pair lubricated with PAO+GMO as a function of the sliding speed compared with those of a needle bearing.

We describe below computer simulations for ta-C finding that 71.5% of the carbon atoms have tetrahedral (sp^3) hybridization and connect to form a percolating 3D interconnected framework. This is corroborated by our XANES experiments [20] and XAES [21] results. Indeed, the XAES spectrum of ta-C coating in the derivative mode shows a fine structure that is assigned to KVV transitions involving π electrons as shown in figure 2. These observations are in good agreement with the works of Mizokawa et al. [22, 23], who indicated, as a fingerprint of the different carbon atoms arrangement, the distance D between the maximum of the positive-going excursion and the minimum of the negative-going excursion in the derivative XAES spectra. The percentage of sp^3 sites in our ta-C coating is thus estimated to 70%. This result is consistent with the high value for hardness (~ 65 GPa) and Young's modulus (650 GPa) we measured by nano-indentation and reported elsewhere [21]. In addition, our DSIMS profiling experiments detected no hydrogen in the bulk of the ta-C coating [21]. A chromium-based interlayer used to improve the adhesion of the ta-C coating to the steel substrate was also detected.

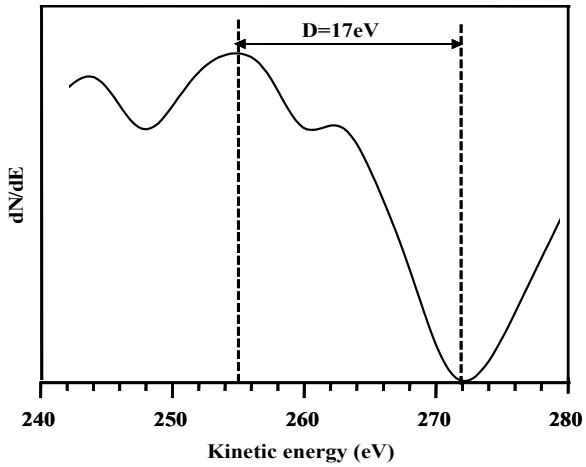

Figure 2: Derivated dN/dE XAES spectrum of ta-C.

Besides the surface sensitive application of AES and XANES, other techniques available for gaining direct imaging and information about changes in the cross-section of the sample were carried out. The Energy Filtered TEM image at 180 eV energy-loss with 7 eV slit width obtained on the FIB cross-section of the ta-C coated steel sample is presented in the figure 3(a). This loss energy permits to diminish the contrast of the image due to the difference between the iron and carbon atomic numbers. This leads to a best visualization of the AISI52100 steel structure and the 30 nm thick chromium-based interlayer previously detected by DSIMS. Notice the metal W layer located above the ta-C coating was necessary for applying the focused ion beam technique. The carbon coating is 730 nm thick and has essentially an amorphous structure. An EFTEM image was performed at 6 eV energy loss, energy corresponding to the π/π^* transition in graphitic carbon, and reported in figure 3(b). In these conditions, a 3 nm thick layer become bright showing the presence of sp^2-bonded carbon at the top surface of the coating. At this stage, our material would be denoted as tetrahedral amorphous carbon or ta-C in the C-H phase diagram terminology of Robertson [24] with an extreme surface (3 nm near to the W layer) richer in graphite-like carbon. This means that there is a chemical heterogeneity of the ta-C coating towards the surface region leading probably to a special surface reactivity in particular in presence of additives molecules.

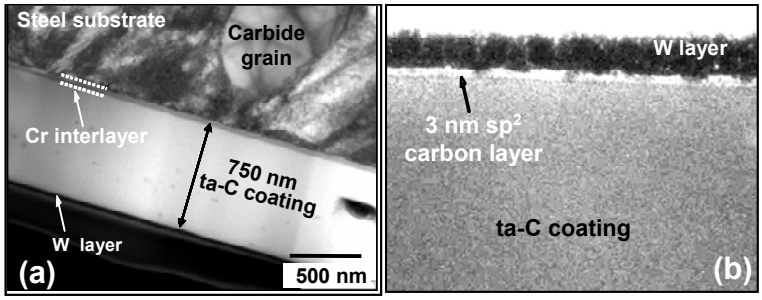

Figure 3: **(a)** EFTEM image at 180 eV energy-loss with 7 eV slit width of a cross-sectioned ta-C coating deposited on a steel substrate and **(b)** EFTEM image at 6 eV energy-loss with 4 eV slit width showing the 3 nm sp^2 carbon layer at the extreme surface of the ta-C coating.

Although the uppermost sliding surface and the underlying area are thought to control macro-scale friction behavior, it is difficult experimentally to estimate shear strength and friction behavior as a function of depth at the nanometer scale [25-28]. Recently, however, we developed a novel nanoscratch method to elucidate the macro-scale effect of reduced friction in relation to the nanoscale tribological properties [29]. The nanoscratch measurements reported in figure 4 show that the sliding area of the ta-C coated steel disc (which exhibits superlow friction in standard pin-on-disc tests) presents low shear strength and low friction coefficients at the nanoscale [29]. Figure 4 also shows the evolution of the nanoscale friction coefficient as a function of scratch depth for inside and outside the wear scar area for the three surface conditions. (1) a non-cleaned surface after the sliding test, (2) a cleaned surface subjected to supersonic cleaning in a hexane solvent and (3) a hexane-cleaned surface rewetted with PAO+GMO oil. The sliding area displayed a lower friction coefficient than the non-sliding area and with an obvious reduction within a depth of less than 5 nm from the surface. This result suggests that a thin tribofilm with low shear strength is formed on the sliding surface of the ta-C disc lubricated with PAO+GMO lubricant. The tribofilm was the reason for the ultralow friction observed for this material combination in the sliding tests. We show below results from the computer simulations consistent with this view.

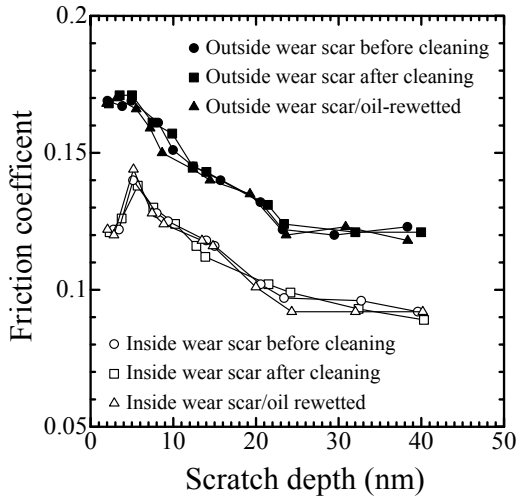

Figure 4: Nanoscratch measurements obtained for three surface conditions in a constant-force nanoscratching process using a conical diamond tip as a stylus for scratching.

3.2. Friction of DLC/DLC in presence of glycerol and GMO

Under boundary lubrication, the mechanism of friction reduction is usually attributed to the effect of long chain polar (amphiphilic) molecules. In the so-called "Self-Assembled Monolayer SAM" or "Monolayer" model, the polar extremity of the molecule is strongly chemisorbed on the native oxide layer present on the steel surface while the paraffinic moitie extends outside the metal surface. The amphiphilic molecules must have at least 10 carbons in their aliphatic chain in order to promote the formation of a crystal-like structure in the SAM layer. Then, low friction is generally attributed to easy sliding of methyl groups over each other, in a way described and also simulated by Molecular Dynamics in the literature by Harrison [30], for example. In our experiments, the SAM model could be applied to GMO since this molecule has a long chain. In order to identify the kind of friction mechanism obtained for ta-C material in presence of OH-containing additives we used pure glycerol which is a short chain molecule containing alcohol chemical functions.

Figure 5 reports the friction coefficients of different material combinations lubricated with PAO+GMO and pure glycerol (G) in a SRV test. Amazing results were obtained for the ta-C/ta-C combination. The friction coefficients of the ta-C couples were substantially lower than for a-C:H/a-C:H and for the steel/steel combinations. These results suggest strongly that the ultra-low friction phenomenon involves the interaction between the ta-C coating and the ester-containing oil due to the formation of a very thin and low-shear-strength tribofilm on the ta-C sliding surface. In addition, these outstanding characteristics of vanishing friction and zero-wear behavior were obtained for the ta-C/ta-C combination lubricated with pure glycerol G at 353 K. As shown in figure 5, the friction coefficient was below 0.01, but the exact value could not be measured with the equipment at hand. Indeed, the wear scar is not visible by optical microscopy. This result suggests that the superlubricity is only related to the alcohol chemical function (OH), which is common to both GMO and glycerol molecules.

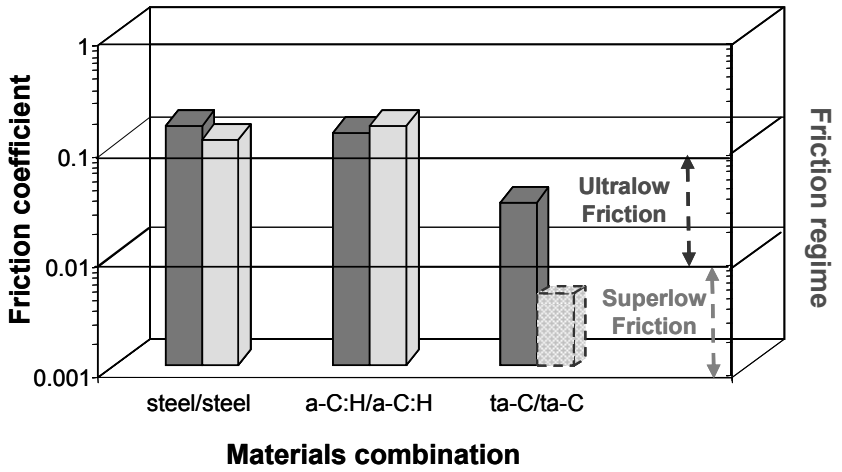

Figure 5: Steady-state friction coefficients obtained in SRV tests of steel/steel and DLC/DLC couples lubricated with PAO+GMO oil in dark gray and with pure glycerol in light gray.

3.3. Computer Simulations to determine the atomistic structures for bulk and surface ta-C DLC

Because of its amorphous character, it has not been possible to determine the detailed 3D structure using experimental methods. Because of its amorphous structure and the long time scales involved with its preparation, it is also quite difficult to predict the structure using first principles quantum mechanics (QM). In order to circumvent these difficulties we developed using the ReaxFF reactive force field [16,

17] based on first principles QM and capable of describing the molecular dynamics (MD) for much larger systems and for much longer times than possible with QM.

Using ReaxFF we predicted 3D structures for the ta-C DLC surface by first melting the a cell of carbon and then quenching to form a glass (details in the METHODS section). We focus here on the 3.24 g/cc system (the experimental value) we denote carbons having 4 single bonds as sp^3, a carbon with bonds to three atoms as sp^2, and a carbon with one or two bonds as sp^1. For the experimental density of 3.24 g/cm^3, we found that 71.5% of the carbon atoms have sp^3 character while 28.1% have sp^2 character and 0.4% atoms have sp^1 character. This is consistent with XAES experimental results, which leads to 70% sp^3 and 30% sp^2. We found that all of the sp^3 atoms interconnect to form a percolating tetrahedral network, to which isolated sp^2 atoms (36%) or short sometimes-branched chains (64%) of sp^2 atoms attach. The sp^1 atoms sometimes lie between two sp^2 atoms (allene) and sometimes are isolated. This structure is shown in figure 6. Here the sp^3 atoms are pink and the sp^2 atoms are blue.

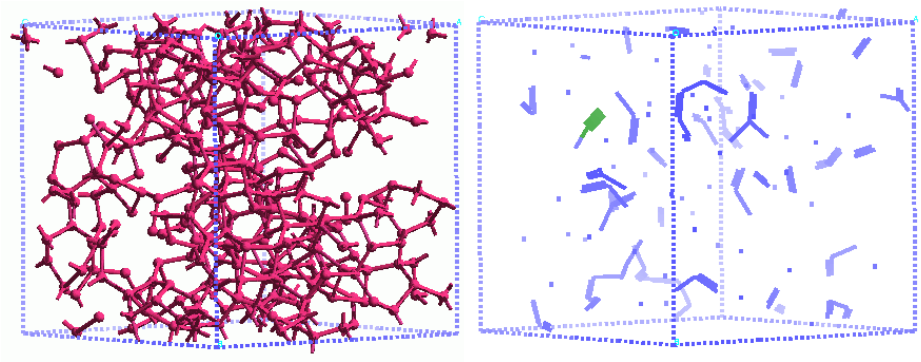

Figure 6: Atomistic 3D structure predicted for bulk DLC with density of 3.24 g/cm^3. Based on ReaxFF MD calculations, quenching from the melt at a cooling rate of 100K/ps.
(A) sp^3 atoms: 71.5% of 512 atoms; they form a percolating tetrahedral network
(B) sp^2 blue atoms: 28.1% and sp^1 green atoms: 0.4%. 36% sp^2 atoms are isolated

To construct the surface of DLC, we cut through the cell along 120 different planes and selected the lowest energy surface. Figure 7 shows the atomic character of the DLC surface formed from DLC bulk system with density of 3.18 g/cm^3 (this has 68% sp^3 and 32% sp^2 atoms). For the DLC surface slab, there are 52% sp^3, 37% sp^2, and 11% sp^1 atoms confirming the stronger sp^2 character of the ta-C top surface shown previously by EFTEM study. About 0.4% of the surface atoms have one bond connected with bulk C atoms.

3.4 Computer Simulations of the frictional properties of lubricated surfaces of ta-C

Using the ta-C surfaces, we carried out MD simulations while sliding the top surface with respect to the bottom one [18, 19]. For the bare surfaces, this leads to very high friction coefficients up to 1.0 and tremendous wear since the unsaturated C atoms at the interface can react by forming and breaking bonds. We then allowed this bare surface to interact glycerol molecules. We introduced 6 glycerol molecules to form a monolayer at the interface. During the sliding, the glycerol reacted with surface C atoms and decomposed. After sliding for 10 ps, we find that 6 H atoms and 4 O-R (OH or other fragments decomposed from glycerol) were adsorbed on the C surface, which did not change over an additional 40 ps. We found that the most active sites for reacting with H or O-R are sp^1 C radical sites. Within the

simulation time (40 ps), we found only one additional sp^2 C atom reacts with H. Figure 8 shows the structure of the simulation model after sliding for 20 ps. Here the atom character after reaction is indicated. The products of decomposition of glycerol were found to be OH, H, O, CH_2O, C_3H_3O, $C_3H_7O_3$, $C_2H_3O_2$, $C_3H_3O_2$. This dramatically reduced the friction coefficient to as low as 0.03 at 0.6 GPa. Thus, hydroxylation on the surface dramatically decreases the friction, leading to ultralow friction. Analyzing the response of the surface atoms during sliding, it appears that the bent C-OH bonds attached to the short sp^1 stubs at the surface make the surface layer very soft (bending the chains rather than compressing bonds) but still elastic, which appears to underlie the superlubricity.

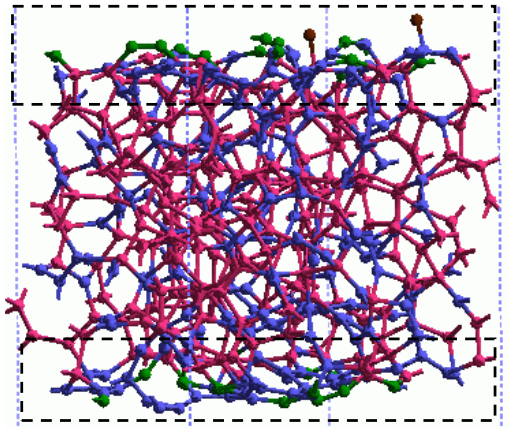

Figure 7: Atomistic 3D structure predicted for the DLC surface (from the bulk system with density of 3.18 g/cm^3). Based on ReaxFF MD calculations. sp^3 (pink): from 68% (bulk) to 52.0% (surface), sp^2 (blue): from 32% (bulk) to 36.7% (surface), sp^1 (green): from 0% (bulk) to 10.9% and there are 2 atoms (0.4%) only have one bond (brown).

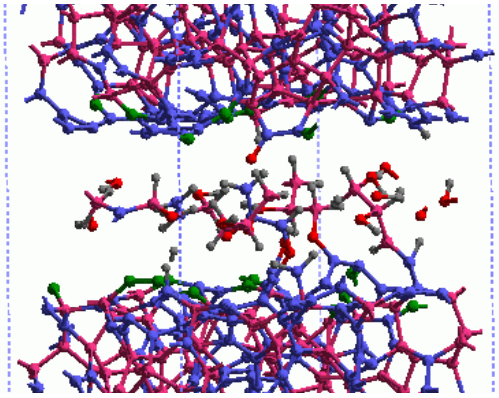

Figure 8: Structure of the glycerol lubricated ta-C after sliding for 20 ps at v=100m/s.
sp^3 C: pink; sp^2 C: blue; sp^1 C: green. O: red; H: gray. There are H and OH species adsorbed on ta-C surfaces and 5 other fragments that are not attached on the surfaces.

3.5. Superlubricity mechanism as studied by ToF-SIMS

To study experimentally the origin of the super low friction observed for glycerol-lubricated ta-C coatings in boundary lubrication, we used surface sensitive molecular analyses technique Time-of-Flight Secondary Ion Mass Spectroscopy (ToF-SIMS). In order to understand the tribochemical reactions that generate the tribofilm (wear track), we used pure ^{13}C glycerol (^{13}C G) and deuterated glycerol (^{2}H G) lubricants. For the ^{13}C glycerol, we substituted ^{13}C for all carbon atoms and in the case of deuterated glycerol only the hydrogen atom of hydroxyl group was substituted.

The friction results obtained with these specific products on ta-C material are very similar to those obtained with standard glycerol [21]. SSIMS spectra were recorded inside and outside the tribofilm area to clarify the material change on the ta-C surface after the super low friction tests. The negative ion spectra

recorded inside and outside the tribofilm formed on ta-C coating after the ^{13}C glycerol lubricated friction test are compared in figure 9 to the spectrum of the virgin ta-C surface. They show clearly the presence of the ^{13}C glycerol molecule ($^{13}C_3H_7O_3^-$) and their characteristic ion fragments ($^{13}C_2H_3O_2^-$, $^{13}CHO^-$, $^{13}CH_2^-$, $^{13}CH_2O^-$) on the ta-C surface after the friction experiment which is consistent with the results of computational simulations reported previously. No higher molecular masses containing ^{13}C obtained by polymerisation of glycerol were found; thus the hypothesis that super low friction results are due to long chain molecules lubrication can be rejected in our case. Also no new species created by the friction were detected inside the tribofilm in comparison with outside. Table 1 reports the relative intensities of the ^{13}C glycerol molecule ($^{13}C_3H_7O_3^-$) and their characteristic ion fragments ($^{13}C_2H_3O_2^-$, $^{13}CHO^-$, $^{13}CH_2^-$, $^{13}CH_2O^-$) versus to the sum of the cluster ion C_n (with $n\geq5$) intensities which are mostly characteristic of ta-C material. The relative intensities of the ^{13}C components were found nearly twice higher inside the wear scar than outside indicating the possible adsorption of glycerol fragments on ta-C surface. Table 1 also reports the relative intensity of the alcohol group (OH). No significant increase was observed for OH group after the friction experiment in comparison with virgin ta-C surface probably due to a tribofilm screening effect and to the strong presence of this specie in the ambient air contamination. However, the super low friction experiments performed with deuterated glycerol (^2H G) lubricant on ta-C coating showed a significant increase in ^2H and O^2H species inside the tribofilm in comparison with outside as shown by the negative ions spectra (figure 10). The ratio between these masses intensities (which are characteristic of deuterated glycerol) and the sum of the cluster ion C_n (with $n\geq5$) intensities was found to be more than twice higher inside the tribofilm, suggesting an hydroxylation of the surface carbon atoms due to frictional processes which leads to a low energy hydrogen interactions between glycerol molecules (and H_2O and other small molecules due to its dissociation under the friction) and hydroxylated ta-C surface.

Table 1: Results of SIMS analysis on DLC surfaces. The relative intensities of the ^{13}C glycerol molecule ($^{13}C_3H_7O_3^-$) and their characteristic ion fragments ($^{13}C_2H_3O_2^-$, $^{13}CHO^-$, $^{13}CH_2^-$, $^{13}CH_2O^-$) versus to the sum of the cluster ion Cn (with $n\geq5$) intensities are presented. The relative intensity of the alcohol group (OH) is also reported. These compositions are consistent with the fragmentation observed in the ReaxFF MD calculations for glycerol lubricated DLC.

	OH	$^{13}CH_2$	^{13}CHO	$^{13}CH_2O$	$^{13}C_2H_3O_2$	$^{13}C_3H_7O_3$	$\Sigma C_{n\geq5}$
Virgin ta-C	883479	NM	NM	NM	NM	NM	100
Inside tribofilm on ta-C	63579	1055	155	118	1488	208	100
Outside tribofilm on ta-C	54534	609	103	69	987	107	100

These experimental results are consistent with the computer simulation results suggesting that the origin of superlubricity in these conditions is attributed to the interaction between two sliding hydroxylated carbon surfaces (OH-terminated carbon film surface).

4. Summary

Summarizing, computer simulations and SIMS experiments confirm the origin of superlubricity of the glycerol lubricated ta-C/ta-C surface and provide an atomic level explanation for the superlubricity in terms of the formation of a low friction tribofilm involving first hydroxylation of surface carbon atoms that occurs upon beginning of the sliding.

The Nissan Engineers have estimated that using this extremely low friction low wear material for the sliding parts in a car engine could reduce fuel consumption of automobiles by 5%. If all automobiles around the world were to use this technology, it could reduce the production of CO_2 by 250 million tons/year.

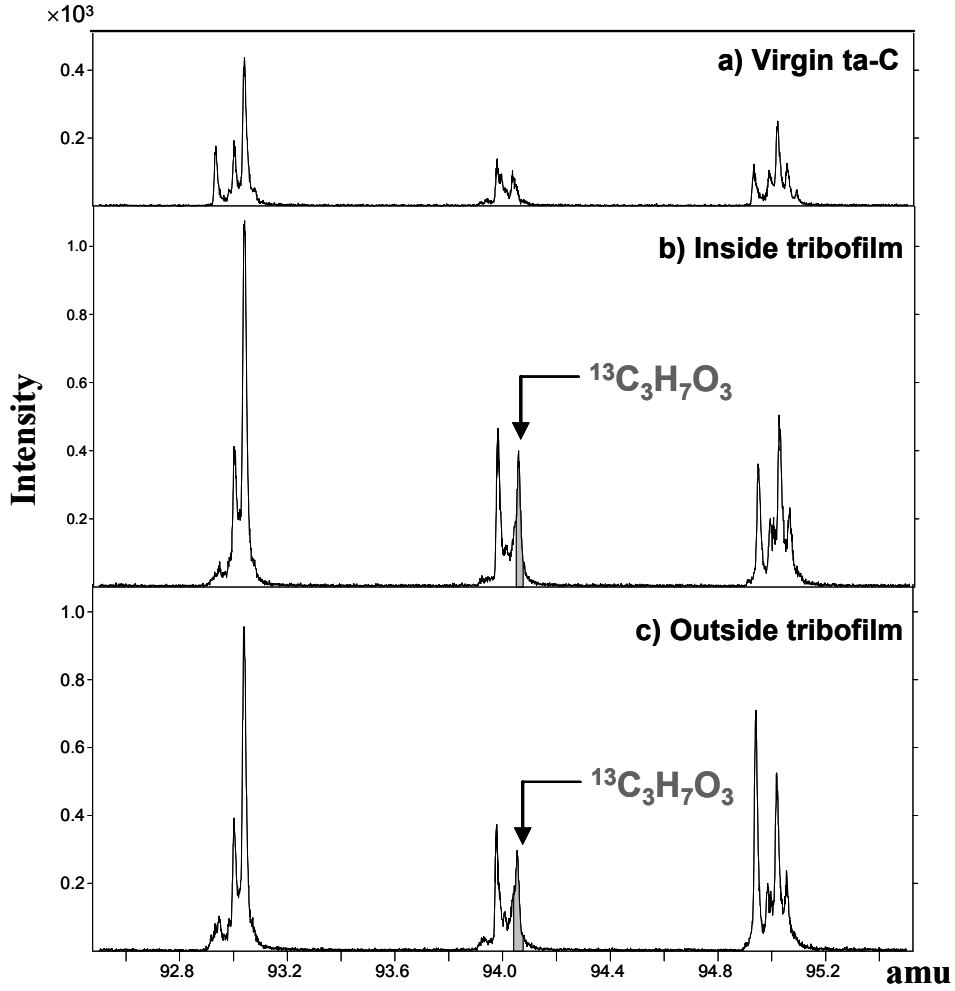

Figure 9: ToF-SIMS surface analyses. **a)** The negative ion spectrum of virgin ta-C surface is compared with spectra obtained **b)** inside the wear track and **c)** outside the wear track after the friction test lubricated with ^{13}C glycerol.

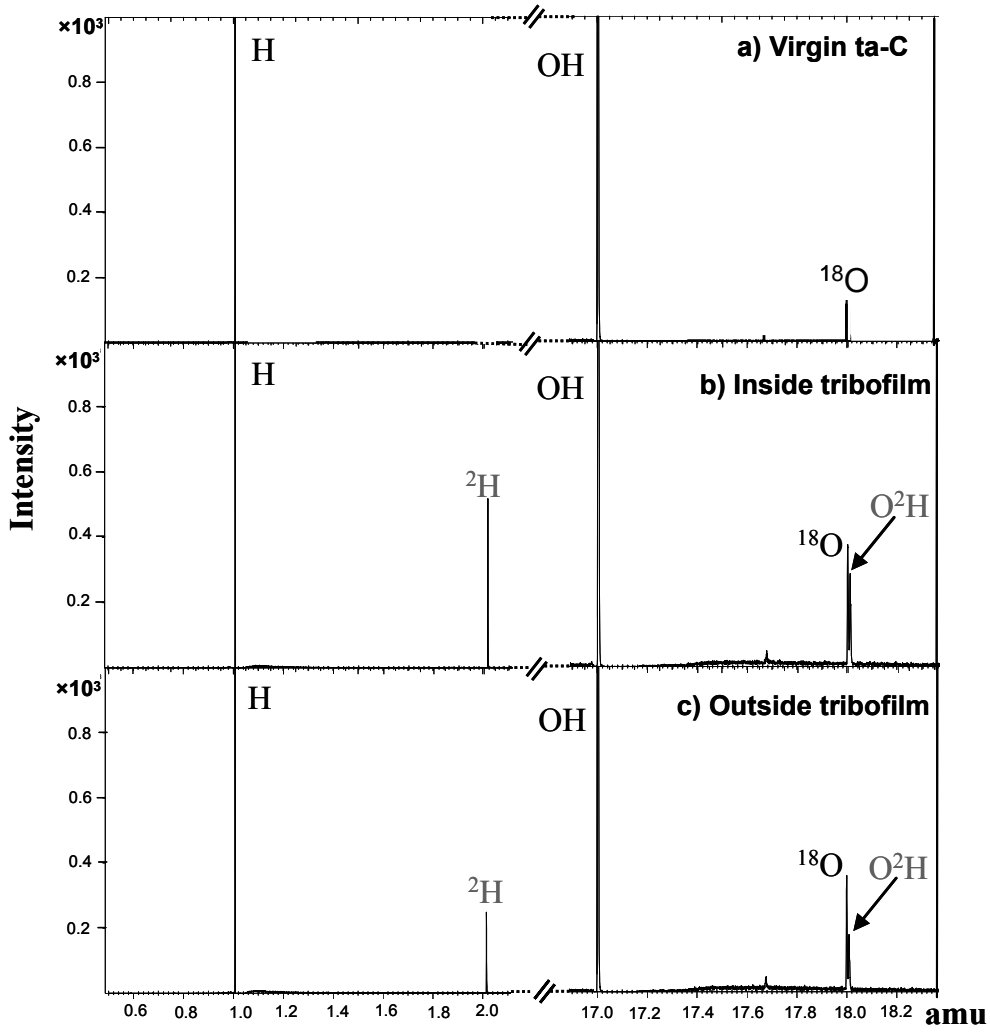

Figure 10: ToF-SIMS surface analyses. **a)** The negative ion spectrum of virgin ta-C surface is compared with spectra obtained **b)** inside the wear track and **c)** outside the wear track after the friction test lubricated with deuterated glycerol.

Acknowledgements
We would like to dedicate this paper to the memory of Dr. Michael Gardos who was instrumental in stimulating our research toward how fundamental chemistry of surfaces plays a role in friction and wear.

References

1. Bowden, F. P. and Tabor, D., 1964 "The friction and Lubrication of Solids, Clarendon Press, Oxford, Part1 pp. 110, Part 2: pp. 158.
2. Bridgeman, P. W., 1936 Proc. Am. Acad. Arts Sci. **7**1 387.
3. Singer, I. LI, Bolster, R. N., Wegang, J. Fayeulle, S., and Stupp, 1990 *Appl. Phys. Lett*. **57** 995.
4. Martin, J. M., Donnet, C., Le Mogne, T., Epicier, T., 1993 Superlubricity of Molybdenum Disulphide, *Physical Review* B **48** N14 10583.
5. Donnet, C., Le Mogne, T., and Martin, J. M., 1993 *Surface and Coatings Technology* **62** 406.
6. Le Mogne, T., Donnet, C., Martin, J. M., Tonck, A., Millard-Pinard, N., Fayeulle, S., and Moncoffre, N., 1994 *J. Vac. Sci. Technol*. A **12** (4) 1998.
7. Martin, J. M., Pascal, H., Donnet, C., Le Mogne, T., and Loubet, J. L., 1994 *Surface and Coatings Technology* **68/69**, 427.
8. Donnet, C., Martin, J. M., Le Mogne, T., and Belin, M., 1996 *Tribology International*, **29**, 2 123.
9. Hirano, M. and Martin, J. M., WTC 97, London, UK, 8-12 September (1997).
10. Chhowalla, M. and Amaratunga, G. A. J., 2000 *Nature* **407**, 164.
11. Donnet C., Fontaine J., Le Mogne T., Belin M., Héau C., Terrat J.P., Vaux F., Pont G., 1999 *Surface and Coatings Technology* **120-121** 548.
12. Heimberg, J., A., Wahl, K., J., Singer, I., L. and Eldemir, A., 2001 *Applied Physics Letters* **78** 17 2449.
13. Gao, F., Erdemir,A., and Tysoe, W.T., 2005 *Tribology Letters* **20** 221.
14. Donnet C., Fontaine J., Grill A., and Le Mogne T., 2000 *Tribology Letters* **9** 137.
15. Fontaine, J., Donnet, C., Grill, A. and Le Mogne, T., 2001 *Surface and Coatings Technology* **146-147** 286.
16. A.C.T. van Duin, S. Dasgupta, F. Lorant and W.A. Goddard, 2001 *J. Phys. Chem. A* **105** 9396.
17. A.C.T. van Duin, A. Strachan, S. Stewman, Q.S. Zhang, X. Xu, and W.A. Goddard III, 2003 *J. Phys. Chem. A* **107** 3803.
18. G.T. Gao, P. T. Mikulski, and J. A. Harrison, 2002 *J. Am. Chem. Soc.* **124** 7202.
19. Q. Zhang, Y. Qi, L. G. Hector, T. Cagin, and W. A. Goddard III, 2005 *Phys. Rev. B* **72** 045406.
20. Kano, M., Yasuda, Y. , Okamoto Y., Mabuchi Y., Hamada T. , Ueno T., Ye, J.,Konishi S., S. Takeshima, Martin J. M., De Barros Bouchet M. I. and Le Mogne, T., 2005 *Tribology Letters*, **18** 245.
21. De Barros Bouchet M. I., Matta C., Le Mogne T, Martin J. M., Sagawa T., Okuda S. and Kano M., 2007 *Tribology-Materials, Surfaces and Interface* **1** 28.
22. Mizokawa Y., Miyasato T., Nakamura S., Geib K.M. and Wilmsen C.W. 1987 *Surf. Sci.* **182** 431.
23. Galuska A.A., Madden H.H. and Allred R.E. 1988 *Appl. Surf. Sci.* **32** 253.
24. Robertson J., Amorphous Carbon: State of the Art, eds. Silva S.R.P., Robertson J., Milne W. and Amaratunga G.A, (Wold Scientific, Singapore, 1998) 32.
25. Warren, O. L., Graham, J. F., Norton, P. R., Houston, J. E. and Milchaske, T. A., Nanomechanical properties of films derived from zinc dialyldithophosphate 1998 Trib. Lett. **4** 189.
26. Graham, J. F., McCague, C. and Norton, P. R., 1999 Trib. Lett. **6** 149.
27. Bec, S., Tonck, A. and Georges, J. M., Coy, R. C., Bell, J. C. and Roper, G. W., 1999 Proc. R. Soc. Lond., A **455** 4181.
28. Mklozic, K. Topolovec, Graham, J., and Spikes, H. A., 2001 Trib. Lett. **11** 71.
29. Ye, J., Kano, M. and Yasuda, Y., 2004 J. Trib. Lett. **16** 107.
30. Harrison, J.A., Gao, G.T., Harrison, R.J., Chateauneuf, G.M., Mikulski, P.T., 2004 Nalwa, H.S. (Ed.), Encyclopedia of Nanoscience and Nanotechnology. Los Angeles, 511.